

Inclusive and diffractive deep inelastic scattering in high-energy QCD *

CYRILLE MARQUET

Service de Physique Théorique, CEA/Saclay
 91191 Gif-sur-Yvette cedex, France
 email: marquet@sph.t.saclay.cea.fr

In the context of both inclusive and diffractive deep inelastic scattering, we derive the first phenomenological consequences of the inclusion of Pomeron loops in the QCD evolution equations towards high energy. We discuss the transition between the well-known geometric scaling regime and the new diffusive scaling, that emerges for sufficiently high energies and up to very large values of Q^2 , well above the proton saturation momentum.

PACS numbers: 12.38.-t, 12.38.Aw, 13.60.Hb, 13.85.-t

1. The Good-and-Walker picture in high-energy QCD

The Good-and-Walker picture [1] of diffraction was originally meant to describe soft diffraction. They express an hadronic projectile $|P\rangle = \sum_n c_n |e_n\rangle$ in terms of hypothetic eigenstates of the interaction with the target $|e_n\rangle$, that can only scatter elastically: $\hat{S}|e_n\rangle = (1 - T_n)|e_n\rangle$. The total, elastic and diffractive cross-sections are then easily obtained:

$$\sigma_{tot} = 2 \sum_n c_n^2 T_n \quad \sigma_{el} = \left[\sum_n c_n^2 T_n \right]^2 \quad \sigma_{diff} = \sum_n c_n^2 T_n^2. \quad (1)$$

It turns out that in the high energy limit, there exists a basis of eigenstates of the large- N_c QCD S -matrix: sets of quark-antiquark color dipoles $|e_n\rangle = |d(r_1), \dots, d(r_n)\rangle$ characterized by their transverse sizes r_i . In the context of deep inelastic scattering (DIS), we also know the coefficients c_n to express the virtual photon in the dipole basis. For instance, the equivalent of c_1^2 for the one-dipole state is the well-known photon wavefunction $\phi(r, Q^2)$ where Q^2 is the virtuality of the photon.

* Presented at the XLVIth Cracow School of Theoretical Physics, Zakopane, Poland, May 27-June 5 2006

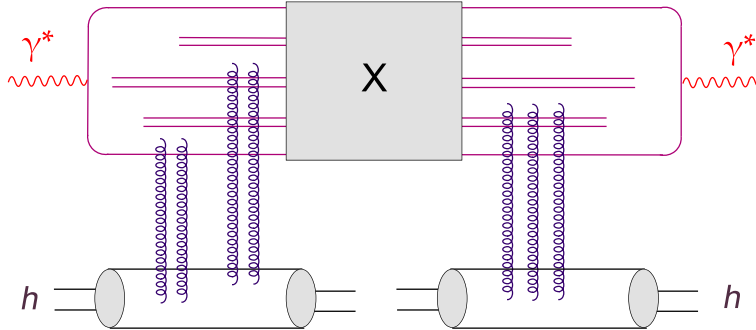


Fig. 1. Representation of the factorization formula (2) for the diffractive cross-section in DIS. The virtual photon is decomposed into dipoles which interact elastically with the target hadron. The rapidity gap is Y_g and the final state X is made of particles produced over a rapidity interval $Y - Y_g$.

This realization of the Good-and-Walker picture allows to write down exact (within the high-energy and large- N_c limits) factorization formulae [2] for the total, elastic and diffractive cross-sections in DIS. They are expressed in terms of elastic scattering amplitudes of dipoles off the target proton $\langle T_n(\{r_i\}) \rangle_Y$, where the average $\langle \dots \rangle_Y$ is an average over the proton wavefunction that gives the energy dependence to the cross-sections ($Y \sim \log(s)$ is the rapidity).

Formulae are similar to (1) with extra integrations over the dipoles transverse coordinates. For instance, denoting the total rapidity Y and the minimal rapidity gap Y_g , the diffractive cross-section reads [2]

$$\sigma_{diff}(Y, Y_g, Q^2) = \sum_n \int dr_1 \cdots dr_n c_n^2(\{r_i\}, Q^2, Y - Y_g) \langle T_n(\{r_i\}) \rangle_{Y_g}^2. \quad (2)$$

This factorization is represented in Fig.1. Besides the Q^2 dependence, the probabilities to express the virtual photon in the dipole basis c_n^2 also depend on $Y - Y_g$. Starting with the initial condition $c_n^2(\{r_i\}, Q^2, 0) = \delta_{1n} \phi(r, Q^2)$, the probabilities can be obtained from the high-energy QCD rapidity evolution. Finally, the scattering amplitude of the n -dipole state $T_n(\{r_i\})$ is given by

$$T_n(\{r_i\}) = 1 - \prod_{i=1}^n (1 - T(r_i)) \quad (3)$$

where $T(r) \equiv T_1(r)$ is the scattering amplitude of the one-dipole state. We are therefore led to study the rapidity evolution of objects such as $\langle T(r_1) \dots T(r_n) \rangle_Y$.

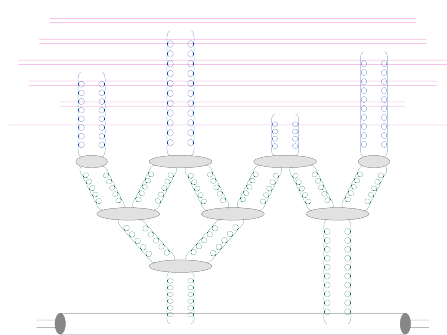


Fig. 2. Elastic scattering of a multiple-dipole state off the target hadron. Shown is a typical contribution included in the Pomeron-loop equation for the amplitudes $\langle T(r_1) \dots T(r_n) \rangle_Y$. In Fig.1, the vertical gluon lines representing the interaction with the hadron actually stand for this type of diagram.

2. The geometric and diffusive scaling regimes

Within the high-energy and large- N_c limits, the dipole amplitudes are obtained from the Pomeron-loop equation [3] (see Fig.2) derived in the leading logarithmic approximation in QCD (see also [4]). This is a Langevin equation which exhibits the stochastic nature [5] of high-energy scattering processes in QCD (see also [6]). Its solution is an event-by-event dipole scattering amplitude function of $\rho = -\log(r^2 Q_0^2)$ and Y (Q_0 is a scale provided by the initial condition). It is characterized by a saturation scale Q_s which is a random variable whose logarithm is distributed according to a Gaussian probability law [7]. The average value is $\log(Q_s^2/Q_0^2) = \lambda Y$ and the variance is $\sigma^2 = DY$ (see Fig.3, left plot). The dispersion coefficient D allows to distinguish between two energy regimes: the geometric scaling regime ($DY \ll 1$) and diffusive scaling regime ($DY \gg 1$).

The following results for the averaged amplitude will be needed to derive the implications for inclusive and diffractive DIS:

$$\langle T(r_1) \dots T(r_n) \rangle_Y \stackrel{Y \ll 1/D}{=} \langle T(r_1) \rangle_Y \dots \langle T(r_n) \rangle_Y , \quad (4)$$

$$\langle T(r_1) \dots T(r_n) \rangle_Y \stackrel{Y \gg 1/D}{=} \langle T(r_<) \rangle_Y , \quad r_< = \min(r_1, \dots, r_n) . \quad (5)$$

All the scattering amplitudes are expressed in terms of $\langle T(r) \rangle_Y$, the amplitude for a single dipole which features the following scaling behaviors:

$$\langle T(r) \rangle_Y \stackrel{Y \ll 1/D}{=} T_{gs}(r, Y) = T(r^2 \bar{Q}_s^2(Y)) , \quad (6)$$

$$\langle T(r) \rangle_Y \stackrel{Y \gg 1/D}{=} T_{ds}(r, Y) = T\left(\frac{\log(r^2 \bar{Q}_s^2(Y))}{\sqrt{DY}}\right) . \quad (7)$$

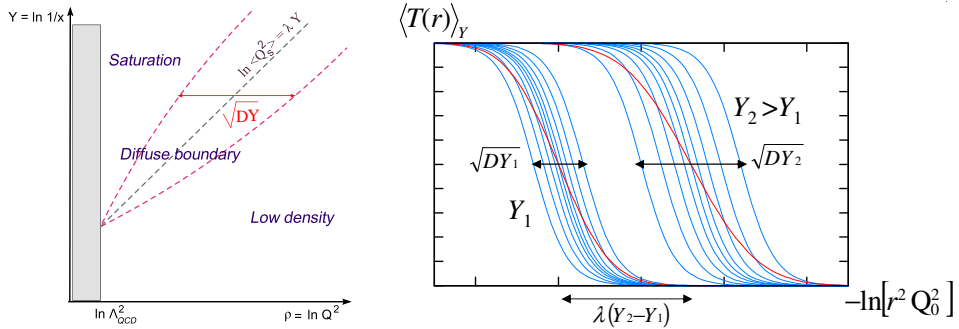


Fig. 3. Left plot: a diagram representing the stochastic saturation line in the (ρ, Y) plane, the diffusive saturation boundary is generated by the evolution. Right plot: different realizations of the event-by-event scattering amplitude (gray curves) and the resulting averaged physical amplitude $\langle T(r) \rangle$ (black curve) as a function of ρ for two different values of Y in the diffusive scaling regime.

In the saturation region $r\bar{Q}_s > 1$, $\langle T(r) \rangle_Y = 1$. As the dipole size r decreases, $\langle T(r) \rangle_Y$ decreases towards the weak-scattering regime, following the scaling laws (6) or (7), depending on the value of DY (see Fig.3, right plot). In the geometric scaling regime ($DY \ll 1$), the dispersion of the events is negligible and the averaged amplitude obeys (6). In the diffusive scaling regime ($DY \gg 1$), the dispersion of the events is important, resulting in the behavior (7).

3. Implications for inclusive and diffractive DIS

We shall concentrate on the diffusive scaling regime, in which the dipole scattering amplitude can be written as follows [8] for $-\log(r^2 \bar{Q}_s^2(Y)) \ll DY$:

$$T_{ds}(r, Y) = \frac{1}{2} \operatorname{Erfc} \left(-\frac{\log(r^2 \bar{Q}_s^2(Y))}{\sqrt{DY}} \right). \quad (8)$$

From this, one obtains the following analytic estimates [2] for the $\gamma^* - p$ total cross-section in DIS and for the diffractive cross-section integrated over the rapidity gap size (at fixed $Y = \log(1/x)$) from $Y_g = \log(1/\beta_<)$ to Y :

$$\frac{d\sigma_{tot}}{d^2 b}(x, Q^2) = \frac{N_c \alpha_{em}}{12\pi^2} \sum_f e_f^2 \sqrt{\pi D \log(1/x)} \frac{e^{-Z^2}}{Z^2}, \quad (9)$$

$$\frac{d\sigma_{diff}}{d^2 b}(x, Q^2, \beta_<) = \frac{N_c \alpha_{em}}{48\pi^2} \sum_f e_f^2 \sqrt{D \log(1/x)} \frac{e^{-2Z^2}}{Z^3}. \quad (10)$$

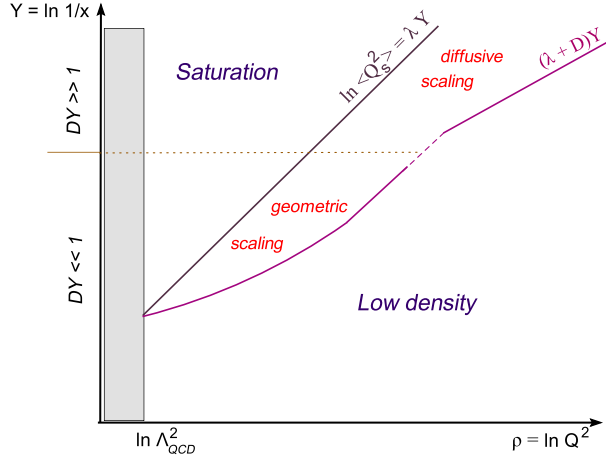


Fig. 4. A phase diagram for the high-energy limit of inclusive and diffractive DIS in QCD. Shown are the average saturation line and the approximate boundaries of the scaling regions at large values of $\rho \sim \ln Q^2$. With increasing Y , there is a gradual transition from geometric scaling at intermediate energies to diffusive scaling at very high energies.

The variable Z is reminiscent of the scaling variable of the dipole amplitude:

$$Z = \frac{\log(Q^2/\bar{Q}_s^2(x))}{\sqrt{D \log(1/x)}}. \quad (11)$$

It shows that in the diffusive scaling regime, both inclusive and diffractive scattering are dominated by small dipole sizes $r \sim 1/Q$. Also the cross-sections do not feature any Pomeron-like (power-law type) increase with the energy and the diffractive cross-section (which does not depend on $\beta_<$) is dominated by the scattering of the quark-antiquark ($q\bar{q}$) component, corresponding to rapidity gaps close to Y . These features a priori expected in the saturation regime ($Q^2 < \bar{Q}_s^2$) are valid up to values of Q^2 much bigger than \bar{Q}_s^2 : in the whole diffusive scaling regime for $\log(Q^2/\bar{Q}_s^2(Y)) \ll DY$ (see Fig. 4).

The inclusive cross-section and the $q\bar{q}$ contribution to the diffractive cross-section are obtained from the dipole amplitude $\langle T(r) \rangle_Y$ in the following way:

$$\frac{d\sigma_{tot}}{d^2b} = 2\pi \int dr^2 \Phi(r, Q^2) \langle T(r) \rangle_Y, \quad (12)$$

$$\frac{d\sigma_{diff}}{d^2b} = \pi \int dr^2 \Phi(r, Q^2) \langle T(r) \rangle_Y^2. \quad (13)$$

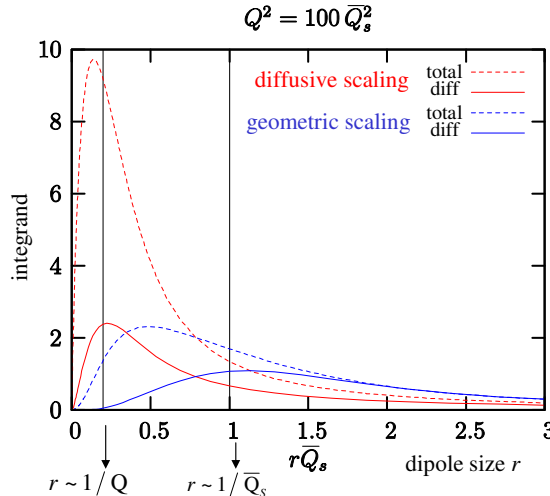


Fig. 5. The integrands of (12) and (13) plotted as a function of $r\bar{Q}_s$ (with $Q/\bar{Q}_s = 10$ fixed) and computed with two expressions for the dipole amplitude: in the geometric and diffusive scaling regimes.

In order to better exhibit the dominance of small dipole sizes $r \sim 1/Q$, we represent in Fig.5 the integrands of (12) and (13) as a function of the dipole size r . Keeping $Q/\bar{Q}_s = 10$ fixed, we use (8) in the diffusive scaling regime and $T_{qs}(r, Y) = 1 - e^{-r^2 \bar{Q}_s^2(Y)/4}$ in the geometric scaling regime.

The difference between the two regimes is striking. In the geometric scaling regime, the total cross-section is dominated by semi-hard sizes ($1/Q < r < 1/\bar{Q}_s$) while the diffractive cross-section is dominated by inverse dipole sizes of the order of the hardest infrared cutoff in the problem: the average saturation scale \bar{Q}_s . In the diffusive scaling regime, both inclusive and diffractive scattering are dominated by inverse dipole sizes of the order of the hardest infrared cutoff in the problem: the hardest fluctuation of the saturation scale, which is as large as Q .

In the diffusive scaling regime, up to values of Q^2 much bigger than the saturation scale \bar{Q}_s^2 , cross-sections are dominated by rare events in which the photon hits a black spot that he sees at saturation at the scale Q^2 . In average the scattering is weak, but saturation is the only relevant physics.

Acknowledgments

The work described here was done in collaboration with Yoshitaka Hatta, Edmond Iancu, Gr  gory Soyez and Dionysis Triantafyllopoulos. I would like to thank the organizers and especially Michal Praszalowicz for giving me the opportunity to present this work at the school.

REFERENCES

- [1] M.L. Good and W.D. Walker, *Phys. Rev.* **120** (1960) 1857.
- [2] Y. Hatta, E. Iancu, C. Marquet, G. Soyez and D. Triantafyllopoulos, *Nucl. Phys.* **A773** (2006) 95;
E. Iancu, C. Marquet and G. Soyez, *Nucl. Phys.* **A** in press, hep-ph/0605174.
- [3] A.H. Mueller, A.I. Shoshi and S.M.H. Wong, *Nucl. Phys.* **B715** (2005) 440;
E. Iancu and D.N. Triantafyllopoulos, *Phys. Lett.* **B610** (2005) 253.
- [4] G. Soyez, these proceedings.
- [5] A.H. Mueller and A.I. Shoshi, *Nucl. Phys.* **B692** (2004) 175;
E. Iancu, A.H. Mueller and S. Munier, *Phys. Lett.* **B606** (2005) 342.
- [6] S. Munier, these proceedings.
- [7] E. Brunet, B. Derrida, A.H. Mueller and S. Munier, *Phys. Rev.* **E73** (2006) 056126;
C. Marquet, G. Soyez and B.-W. Xiao, hep-ph/0606233.
- [8] E. Iancu and D.N. Triantafyllopoulos, *Nucl. Phys.* **A756** (2005) 419;
C. Marquet, R. Peschanski and G. Soyez, *Phys. Rev.* **D73** (2006) 114005.